
Article:
Zhao, Y, Zhang, Z, Li, Z et al. (2020) An EMG-driven musculoskeletal model for estimating continuous wrist motion. IEEE Transactions on Neural Systems and Rehabilitation Engineering. ISSN: 1534-4320

https://doi.org/10.1109/tnsre.2020.3038051

An EMG-driven musculoskeletal model for estimating continuous wrist motion

Yihui Zhao, Zhiqiang Zhang, *Member, IEEE,* Zhenhong Li, Zhixin Yang, *Member, IEEE,* Abbas A. Dehghani-Sanij and Sheng Q. Xie, *Senior Member, IEEE*

***Abstract*—EMG-based continuous wrist joint motion estimation has been identified as a promising technique with huge potential in assistive robots. Conventional data-driven model-free methods tend to establish the relationship between the EMG signal and wrist motion using machine learning or deep learning techniques, but cannot interpret the functional relationship between neuro-commands and relevant joint motion. In this paper, an EMG-driven musculoskeletal model is proposed to estimate continuous wrist joint motion. This model interprets the muscle activation levels from EMG signals. A muscle-tendon model is developed to compute the muscle force during the voluntary flexion/extension movement, and a joint kinematic model is established to estimate the continuous wrist motion. To optimize the subject-specific physiological parameters, a genetic algorithm is designed to minimize the differences of joint motion prediction from the musculoskeletal model and joint motion measurement using motion data during training. Results show that mean root-mean-square-errors are 10.08°, 10.33°, 13.22° and 17.59° for single flexion/extension, continuous cycle and random motion trials, respectively. The mean coefficient of determination is over 0.9 for all the motion trials. The proposed EMG-driven model provides an accurate tracking performance based on user's intention.**

***Index Terms*—Hill's muscle model, Electromyogram signal, Forward dynamics, Continuous wrist joint motion.**

I. Introduction

ESTIMATING human joint motion is critical for the human-machine interfaces (HMIs) that can respond to users' intentions accurately and promptly [1]. Electromyogram (EMG) signal based HMIs show great advantages in the estimation of human intension: 1) using non-invasive electrodes to capture EMG can interpret the muscle activities precisely; 2) EMG signal can be detected ahead of actual motion about 10 - 100 ms, which enables estimate intended action in real-time [2]; 3) EMG-based HMIs allow users to control the assistive robot more intuitively and smoothly [3].

This work was supported in part by the Engineering and Physical Sciences Research Council of U.K. under Grant EP/S019219/1. (Corresponding author: Sheng Q. Xie.)

Yihui Zhao, Zhiqiang Zhang, and Zhenhong Li are with the School of Electronic and Electrical Engineering, University of Leeds, Leeds LS2 9JT, U.K (e-mail: el14yz@leeds.ac.uk; Z.Zhang3@leeds.ac.uk; z.h.li@leeds.ac.uk).

Abbas A. Dehghani-Sanij is with the School of Mechanical Engineering, University of Leeds, Leeds LS2 9JT, U.K (email: A.A.Dehghani-Sanij@leeds.ac.uk).

Sheng Q. Xie is with the School of Electronic and Electrical Engineering, University of Leeds, Leeds LS2 9JT, U.K., also collaboration with the Institute of Rehabilitation Engineering, Binzhou Medical University, Yantai 264033, China. (email: s.q.xie@leeds.ac.uk)

Zhixin Yang is with the Electromechanical Engineering University of Macau, Macau, China. (e-mail: zxyang@um.edu.mo)

EMG based continuous limb motion estimation approaches can be categorized into two subsets, model-free and model-based. For model-free approaches, they involve machine learning techniques, mapping the relationship between EMG signals and the desired motion by the numerical functions. Several artificial neural network methods are applied to estimate continuous motion in the human upper limb. For example, Lei proposed a back-propagation neural network to estimate continuous elbow motion [4], and U. Côté-Allard *et al.,* have developed a deep learning algorithm to recognise hand gestures [5]. Nevertheless, model-free approaches have some limitations. It is a 'black box' method, employing a general map function rather than explicitly revealing the functional relationships between neuro-commands and the corresponding motion. A large amount of data sets containing EMG signals as well as the related motions is required to train the transfer function in order to interpret the prediction with given EMG signals. Additionally, model-free approaches may not be able to respond to novel motions that are not defined in the training set [6].

To provide the explicit representation between the EMG signal and joint kinetic and kinematic characteristics and reduce the acquirement of training data, model-based approaches have been widely applied to establish the HMIs. These approaches estimate the continuous limb motion through an EMG-driven musculoskeletal model. For example, Pau *et al.,* proposed a simplified geometric model together with a musculoskeletal model to estimate the continuous motion of the elbow joint [7]. A musculoskeletal model was employed to simulate the shoulder and elbow joint motion in real-time using a passive damper to avoid the numerical stiffness [8]. Blana *et al.,* proposed the implicit formulation of the musculoskeletal model in order to drive the wrist/hand motion in real-time [9]. However, their models' parameters are adapted from the existed biomechanical models and have not taken the subject-specificity into account. Crouch *et al.,* proposed a musculoskeletal model using subject-specific parameters to estimate the flexion/extension motion of wrist joint and metacarpophalangeal (MCP) joint [10]. Nevertheless, using few muscles to establish the musculoskeletal model may overestimate the physiological parameters, i.e., the parameters may exceed the physiological range when these muscles are assumed to be the only muscle groups contributing to the joint motion. In [10], the subject-specific parameters exceeded the physiological range largely, because they have only used two wrist muscles to estimate the wrist flexion/extension motion.

In this paper, we propose a model-based approach to esti-

mate the wrist continuous joint motion. The main contributions of this paper include: 1) five primary wrist muscles are grouped into flexor/extensor to avoid over-estimating parameters; 2) according to the selected muscle groups, a musculoskeletal model including a muscle-tendon model and a joint kinematic model is derived to estimate the continuous wrist flexion/extension motion. Assuming the tendon is rigid, the numerical stiffness of the muscle-tendon model is alleviated; 3) a parameter optimization algorithm is designed and implemented to tune the parameters within the physiological range by minimizing the differences of joint motion between the model's estimation and the measured data. Results show the proposed approach can estimate the wrist flexion/extension motion accurately.

The remaining paper is arranged as follows. Experiment protocol is described in section II-E, and the results are concluded in section III. Section IV discusses the performance and the limitations of the proposed model. Final section gives conclusion and future work.

II. Methods

In the single degree of freedom (DoF) configuration, five primary wrist muscles are grouped into wrist flexor-extensor. The flexor digitorum superficialis (FDS) and extensor digitorum (ED) are excluded due to these muscles mainly contribute to the MCP motion. Therefore, the five main wrist muscles ($i = 1, 2, \ldots, 5$) are described in following: 1) Flexor ($i = 1, 2$) includes Flexor Carpi Radialis (FCR) and Flexor Carpi Ulnaris (FCU); 2) Extensor ($i = 3, 4, 5$) includes Extensor Carpi Radialis Longus (ECRL), Extensor Carpi Radialis Brevis (ECRB) and Extensor Carpi Ulnaris (ECU). The wrist joint motion is computed by a muscle activation interpretation method, a muscle-tendon model and a joint kinematic modelling technique. Muscle activation interpretation method computes the muscle activation levels from EMG signals. The muscle-tendon model estimates the muscle-tendon force regarding the force-length/velocity relationships and muscle activation levels, based on the Hill's muscle modelling technique. Then the joint kinematic modelling technique is developed to determine the muscle tendon length and moment arms against joint angle and computes the joint motion using forward dynamics. A parameter optimization algorithm is developed to tune the physiological parameters. In the rest of this section, we will explain how to estimate the wrist joint motion using the proposed model.

A. Muscle activation interpretation method

To interpret the muscle activation level of each muscle during the wrist motion, the raw EMG signals are processed through a non-linear equation. The raw EMG signals are first filtered by a 2^{nd} order Butterworth band-pass filter at cut-off frequencies between 25 Hz and 450 Hz to remove baseline and artefact noise, and then fully rectified. The rectified signals are low-pass filtered to clarify the characteristics of EMG to muscle force relation using 4^{th} order Butterworth low-pass filter at a corner frequency of 4 Hz. Filtered signals are normalized by dividing the peak value of isometric maximum voluntary contraction (IMVC). The following equation is account for the non-linear relationship between pre-processed signal $u_i(t)$ and muscle activation $a_i(t)$ in each muscle

$$a_i(t) = \frac{e^{Au_i(t)} - 1}{e^A - 1} \tag{1}$$

where non-linear shape factor *A* has the range of highly non-linearity (-3) to linearity (0.01) [11].

B. Muscle-tendon model

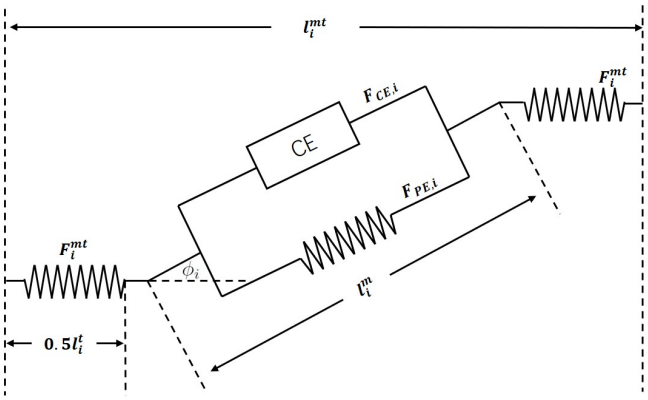

Fig. 1: Schematic of Hill's type muscle model.

The Hill's modelling technique is used to compute the muscle-tendon force F_i^{mt}, which consists of a elastic tendon in series with a muscle fibre. The muscle fibre includes a contractile element (CE) in parallel with passive elastic element. l_i^{mt}, l_i^m and l_i^t are the muscle-tendon length, muscle fibre length and tendon length respectively. Pennation angle ϕ_i is the angle between the orientation of the muscle fibre and tendon, and the pennation angle at current muscle fibre length is calculated by

$$\phi_i = \sin^{-1}\left(\frac{l_{o,i}^m \sin\phi_{o,i}}{l_i^m}\right) \tag{2}$$

where $l_{o,i}^m$ and $\phi_{o,i}$ represent the optimal muscle fibre length and the optimal pennation angle respectively. Besides, a scale coefficient k_i^{mt} is introduced to account the difference of the muscle-tendon length across subjects. The muscle fibre length is represented as

$$l_i^m = (k_i^{mt} l_i^{mt} - l_i^t)\cos^{-1}\phi_i. \tag{3}$$

The F_i^{mt} is the summation of the active force $F_{CE,i}$ and the passive force $F_{PE,i}$, which can be written as

$$F_i^{mt} = (F_{CE,i} + F_{PE,i})\cos\phi_i. \tag{4}$$

The $F_{CE,i}$ is the active force generated by CE, which can be written as

$$F_{CE,i} = F_{o,i}^m f_a(\bar{l}_{i,a}^m) f(\bar{v}_i) a_i(t) \tag{5}$$

where $F_{o,i}^m$ is the maximum isometric force. The function $f_a(\cdot)$ represents the active force-length relationship at different muscle fibre length and muscle activations, which is written as

$$f_a(\bar{l}_{i,a}^m) = e^{-(\bar{l}_{i,a}^m - 1)^2 k^{-1}} \tag{6}$$

where the $\bar{l}^m_{i,a} = l^m_i/(l^m_{o,i}(\lambda(1-a_i(t))+1)$ is the normalized muscle fibre length with respect to the corresponding activation levels and λ is a constant, which is set to 0.15 [12]. The k is a constant to approximate the force-length relationship, which is set to 0.45 [13]. The function $f(\bar{v}_i)$ represents the force-velocity relationship between the l^m_i and the normalized contraction velocity $\bar{v}_i$ [14]

$$f(\bar{v}_i) = \begin{cases} \frac{0.3(\bar{v}_i+1)}{-\bar{v}_i+0.3} & \bar{v}_i \leq 0 \\ \frac{2.34\bar{v}_i+0.039}{1.3\bar{v}_i+0.039} & \bar{v}_i > 0 \end{cases} \tag{7}$$

where $\bar{v}_i = v_i/v_{o,i}$. $v_{o,i}$ represents the maximum contraction velocity, which is set to 10 $l^m_{o,i}$/sec [15]. The v_i is the derivative of the muscle fibre length. Note that the passive force F_{PE} is the forced produced by the passive elastic element which can be calculated as

$$F_{PE,i} = \begin{cases} 0 & l^m_i \leq l^m_{o,i} \\ f_p(\bar{l}^m_i)F^m_{o,i} & l^m_i > l^m_{o,i} \end{cases} \tag{8}$$

where $\bar{l}^m_i = l^m_i/l^m_{o,i}$ is the normalized muscle fibre length. The $f_p(\cdot)$ is

$$f_p(\bar{l}^m_i) = \frac{e^{10(\bar{l}^m_i-1)}}{e^5}. \tag{9}$$

C. Joint kinematic modelling technique

The single joint configuration is presented to estimate the wrist continuous joint motion. The muscle-tendon length l^{mt}_i and moment arm r_i against wrist joint angle are calculated using the polynomial equation and the scale coefficient [16]. The joint torque of each muscle can be calculated as

$$M_i = F^{mt}_i r_i. \tag{10}$$

Therefore, the total joint torque during wrist motion is written as

$$\tau = \sum_{i=1}^{2} M_{flexor,i} - \sum_{i=3}^{5} M_{Extensor,i} \tag{11}$$

where $M_{flexor,i}$ and $M_{extensor,i}$ represent the flexor torque and extensor torque, respectively.

Since the muscle activation level does not have a directly relationship with the joint motion, it is necessary to compute joint acceleration using the forward dynamics (Fig. 2). The wrist joint is assumed to be a single hinge joint, the palm and fingers are assumed to be a rigid segment rotating around wrist joint in the sagittal plane. Thus, we can have the following relationship based on the Lagrange equation

$$\ddot{\theta} = \frac{\tau - mgL\sin(\theta) - C\dot{\theta}}{I} \tag{12}$$

where $\ddot{\theta}$ is the angular acceleration. τ is derived from (11). I is the moment of inertia of hand, which is equal to $mL^2 + I_p$. I_p is the moment of inertia at the principal axis which is parallel to the flexion/extension axis [17]. m and L are the mass of hand and the length between rotation centre to hand's centre of mass, which are measured from subjects. θ and $\dot{\theta}$ are the wrist joint angle and angular velocity respectively. C is the damping coefficient representing the elastic and viscous effects from tendon, ligaments. Therefore, the EMG-based model for the wrist joint motion estimation in discrete time can be written as

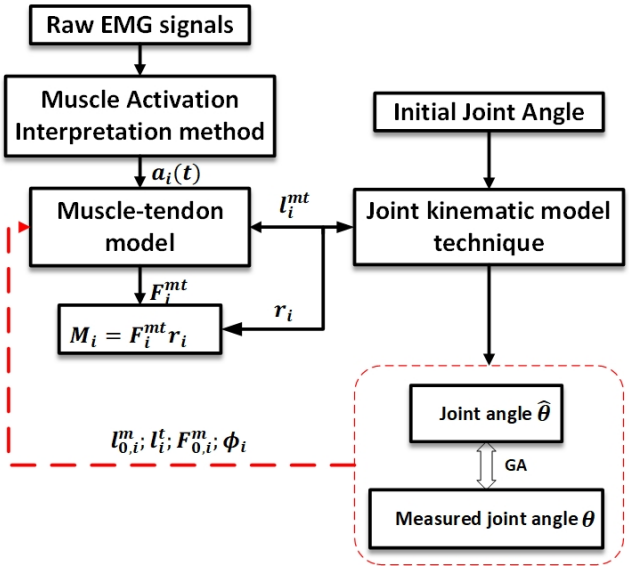

Fig. 2: Joint motion update flowchart: muscle activation interpretation methods gives muscle activation levels of each muscle, muscle-tendon force is computed by a muscle-tendon model, and the joint kinematic model estimates the wrist joint motion θ. The physiological parameters, e.g,. optimal muscle fibre length $l^m_{o,i}$, tendon length l^t_i, maximum muscle force $F^m_{o,i}$ and optimal pennation angle ϕ_i are optimized using the GA algorithm.

$$\dot{\theta}_{t+1} = \dot{\theta}_t + \ddot{\theta}_t \Delta t \tag{13}$$

$$\theta_{t+1} = \theta_t + \dot{\theta}_t \Delta t \tag{14}$$

where Δt is the sampling time, and $\dot{\theta}_t$ and θ_t are the angular velocity and joint angle at time t.

D. Parameter optimization algorithm

The muscle-tendon parameters in the proposed model, e.g., maximum isomeric muscle force, optimal fibre length, tendon length and optimal pennation angle are difficult to measure in *vivo* and varies between the age, gender [18]. Thus, these parameters are required to be optimized for each subject. The initial guess and the physiological boundaries of the muscle-tendon parameters are chosen according to [19] and [20], which are presented in Table I. The boundaries of maximum isometric force are set to $\pm 50\%$ of the initial guess since the variation of the physiological cross-sectional area are varied between subjects. Genetic algorithm (GA) is used to find out the best match of the subject-specific parameters. The parameter vector is represented as

$$\chi = [F^m_{o,i}, l^m_{o,i}, l^t_{o,i}, \phi_i, k^{mt}_i, A]^T \tag{15}$$

The estimation of χ can be written as

$$\hat{\chi} = \arg\min_{\chi}\{f(\chi)\} \tag{16}$$

where

$$f(\chi) = \sqrt{\frac{1}{N}\sum_{n=1}^{N}(\theta - \hat{\theta})} \tag{17}$$

where θ and $\hat{\theta}$ are the measured joint angle and estimated joint angle respectively, and N is the number of samples.

GA is commonly implemented in the musculoskeletal model [7]. It can evaluate multiple solutions in the search space, and reduce the risk of falling into a local minima. GA mimics the nature evolutionary process by representing the muscle-tendon parameters as a 'chromosome'. The algorithm randomly generates a set of possible solutions for the joint kinematic modelling technique. The objective function evaluates the "fitness" of each possible solution at each generation and reaches the best set of parameters iteratively.

TABLE I: Boundaries of parameters

Parameters (units)	**Bounds**
Maximum isometric muscle force $F^m_{o,i}$ (N)	[initial guess$\pm$50%]
Optimal muscle fibre length $l^m_{o,i}$ (m)	[initial guess$\pm$0.010]
Tendon length l^t_i (m)	[initial guess$\pm$0.010]
Optimal pennation angle $\phi_{o,i}$ (rad)	[initial guess$\pm$5%]
Non-linear shape factor A	[-3,0.01]
Scale coefficient k^{mt}_i	[0.9,1.2]

Furthermore, a sensitivity analysis is conducted to investigate the sensitivities of the model output to the optimized muscle-tendon parameters, which can be calculated by [21]:

$$SI_j = \frac{(M_{j,pret} - M_{opt})/M_{opt}}{(P_{j,pret} - P_{j,opt})/P_{j,opt}} \tag{18}$$

where $M_{j,pret}$ and M_{opt} represent the perturbed model output and optimal model output respectively. $P_{j,pert}$ and $P_{j,opt}$ are the j^{th} perturbed parameter and the j^{th} optimized parameter in the proposed model respectively. Additionally, the muscle-tendon lengths and moment arms are also considered. The maximum isometric forces are perturbed by $\pm 20\%$ and other parameters are perturbed by $\pm 10\%$. The sensitivity coefficient SI_j is used for comparison between parameters.

E. Experiment

The experiment is approved by the MaPS and Engineering Joint Faculty Research Ethics Committee of the University of Leeds (MEEC 18-002). Eight subjects participate in this experiment (six males and two females), between the age of 25 and 31. The consent forms are signed by all subjects. We take the subject's weight data and the length of their hand in order to calculate the moment of inertia of the hand.

1) EMG data acquisition: Delsys Trigno^{TM} system is used to record the raw EMG signals. The placement of electrodes is placed following SENIAM recommendation [22]. The sampling rate of EMG signals is 2000 Hz. Avanti electrodes are placed over five wrist muscles over right forearm, according to section II.

Fig. 3: Neutral Position: 16 reflective markers are attached on subject's right upper limb. Electrodes are placed on five primary muscles of wrist joint, including FCR, FCU, ECU, ECRL and ECRB.

2) Motion Capture system: The trajectory data is captured through the motion capture system (VICON Motion Systems Ltd. UK) at 250 Hz. 16 reflective markers are placed on the subject's right upper limb. Markers are allocated over the spinous process of the 7^{th} and the 10^{th} thoracic vertabra, right scapula, xiphoid, acromio-clavicular joint, clavicle, lateral/medial humerus medial epicondyle, right radial/ulnar styloid, middle forearm and the right third metacarpus. The kinematic data and EMG data are synchronized using a trigger module via the VICON nexus software. The wrist joint angle is computed from VICON upper limb model [23].

3) Experiment setup: Subjects are asked to seat on the armchair while torso is fully straight, right shoulder is abducted at 90° and elbow is flexed at 90°, as shown in Fig. 3. Their forearm and hand are fully relaxed and the position of hand is set as the neutral position ($\theta = 0°$). The subject's arm is shaved and skin is cleaned up using an alcohol wipe in order to minimize the artefact and impedance of the electrodes. Before the experiment, the IMVC and the static anatomical posture of each subject are recorded. Four sets of wrist movement are performed whilst the MCP joint is keeping full extension to reduce the effect of wrist muscles during the experiment. Furthermore, the subjects are informed to try to avoid the ulnar/radial deviation and the experimental data with radial/ulnar deviation are excluded.

The wrist motion trials include: 1) flexion motion, which move the wrist towards to the palm side and then return to neutral position. 2) extension motion, which starts from neutral position, move the wrist towards to the back-hand side and then return to neutral position. 3) continuous cycle motion requires to perform consecutive wrist flexion/extension motion. Starting from neutral position, and then move the wrist to either flexion/extension direction, and finally return to neutral position. 4) Random motion is based on the subject's intention. They are asked to move their wrist freely in varying amplitudes and at varying speed. The resultant motion data are low-pass filtered and set as the reference. Five repetitive trials are performed for each movement and a three minute break is given between each trial to prevent muscle fatigue. The first continuous cycle trial is selected as a training trial to

optimize the parameters. The remaining four continuous cycle motion trials and all flexion/extension motion and random motion trials are used for validation. Each flexion/extension motion trial and the training trial lasts for 2-5 seconds while the continuous cycle/random motion trial lasts for about 15-20 seconds.

III. Results

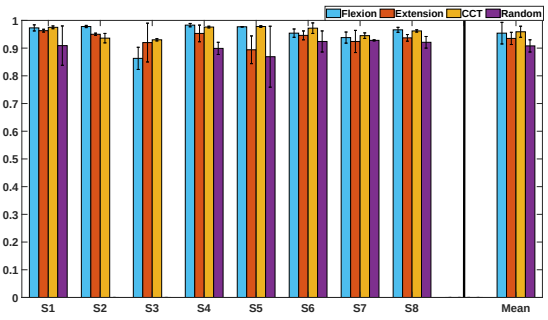

Fig. 4: Mean R^2 across subjects in the flexion (mean $R^2 = 0.95$), extension (mean $R^2 = 0.94$), continuous cycle motion (CCT, mean $R^2 = 0.96$) and random motion (mean $R^2 = 0.91$) with the standard deviation.

A. Verification of EMG-driven model

The proposed model is verified by the validation sets using the root-mean-square-error (RMSE) and the coefficient of determination (R^2). RMSE and R^2 indicate the difference in terms of amplitude and correlation between the estimated joint angles/velocities and reference respectively. Table II and Fig. 4 summarizes the mean RMSEs and R^2 of the experimental motion trials across all subjects. The random motion trials of subject 2 and subject 3 are excluded due to the unacceptable noise captured in the experiment. In this study, the mean RMSE and R^2 of the random motion trials are calculated using the remaining subjects' data.

1) Predefined motion: The results of one single flexion/extension and one continuous cycle trial of subject four are illustrated in Fig. 5. In each subfigure, joint angle (top panel) and joint velocity (bottom panel) denote the estimated results compared with the reference. The results of the single flexion/extension trials indicate the model can estimate the correct motion according to the measured EMG signals. Furthermore, the results of the pre-defined trials shows the proposed model with the optimized muscle-tendon parameters can estimate the wrist flexion/extension motion accurately.

2) Random motion: The results of random motion trials denote that the proposed model can provide the accurate estimation in trend (mean $R^2 = 0.91$), but the amplitudes deviate from the reference (mean $\mathrm{RMSE} = 17.59°$). Additional estimation performance of subject six and eight are illustrated in Fig. 6 and Fig. 7, respectively.

B. Parameters Identification

The subject-specific parameters are identified by GA. Table III presents the variation of the optimized parameters together with the initial guess (left column) of subject five. The deviations of the optimal fibre length, tendon length, optimal pennation angle and muscle-tendon length scaler are small from the initial guess (max 7.46% in ECRL). The maximum isometric forces deviate largely from the initial value. The optimized non-linear shape factor A is -2.716. To evaluate the sensitivities of the optimized parameters, the results of the sensitivity analysis of subject five is presented in Fig. 8. The sensitivity coefficient of the non-linear shape factor A is 0.3134.

IV. Discussion

1) Model's performance: In this paper, the experiments are conducted to evaluate the accuracy and tracking performance of the proposed model for the estimation of the continuous wrist joint flexion/extension motion. The estimated joint angles of all motion trials are highly correlated to the reference elucidate that the proposed EMG-driven model can respond to the subjects' intention accurately according to the given EMG signals. The EMG-driven model shows its capability to maintaining high performance (mean R^2 = 0.91) in terms of the varying rotating velocities and different range of motions.

The RMSEs are similar in the single flexion/extension trials but increase in the continuous cycle motion and random motion trials. The estimation errors may be caused by the crosstalk and the muscle co-activation that generates small muscle force during the wrist flexion/extension motion. Recently, high-density surface EMG is used to collect the high-resolution signals over the forearm. Therefore, the spatial distribution of the muscle activities can be identified and clustered to increase the fidelity of the EMG signals [24]. Furthermore, the passive tendon force is largely different in wrist flexion/extension motion which also results in estimation errors. Nevertheless, it is preferred to estimate the joint motion with greater R^2 rather than the RMSE for the application of EMG-based HMIs in assistive robots [25]. This is because the EMG-driven musculoskeletal is an open-loop estimation model. In practical, the close-loop control strategies are employed in HMIs. The estimation errors can be reduced through adding feedback signals, e.g., using a Kalman filter [26] or an error estimation model [27]. Furthermore, the proprioceptive output from the muscle spindle model or the force feedback from the Glogi tendon organ model may also have potential as the feedback signals in the EMG-driven model [28].

2) Comparison with literature: The proposed model is compared with the models [7] and [10], which estimate the singe degree-of-freedom joint motion through the open-loop musculoskeletal model. The proposed model shows better performance in the continuous cycle motion and random motion compared with [7], whose method has the mean RMSEs of 22° and 22.4° for continuous cycle motion and random motion respectively. The mean RMSE of single elbow flexion/extension is smaller than the proposed model. However, they have tuned each trial four times and selected the smallest RMSE. The

TABLE II: Mean RMSE (deg) in validation trials

	Subjects																	
	S1		S2		S3		S4		S5		S6		S7		S8		Total	
Motion trial	**Mean**	**Std.**	**Mean**	**Std.**	**Mean**	**Std.**	**Mean**	**Std.**	**Mean**	**Std.**	**Mean**	**Std.**	**Mean**	**Std.**	**Mean**	**Std.**	**Mean**	**Std.**
Flexion	12.49	1.11	3.54	0.91	12.71	3.05	9.59	2.66	8.08	2.23	6.50	1.48	16.91	2.32	10.80	1.66	**10.08**	**4.13**
Extension	14.39	6.57	8.50	5.14	7.93	2.55	9.01	2.00	10.27	1.90	15.85	5.49	9.03	0.91	7.69	0.75	**10.33**	**3.08**
Continuous Cycle	13.48	1.70	14.15	3.51	9.40	1.15	15.64	3.61	8.59	1.38	15.47	2.97	15.50	2.58	13.25	1.88	**13.22**	**2.77**
Random	15.06	1.72	Null		Null		14.94	5.38	26.63	8.77	17.79	4.85	12.99	0.42	18.13	1.00	**17.59**	**4.41**

Std. = standard deviation

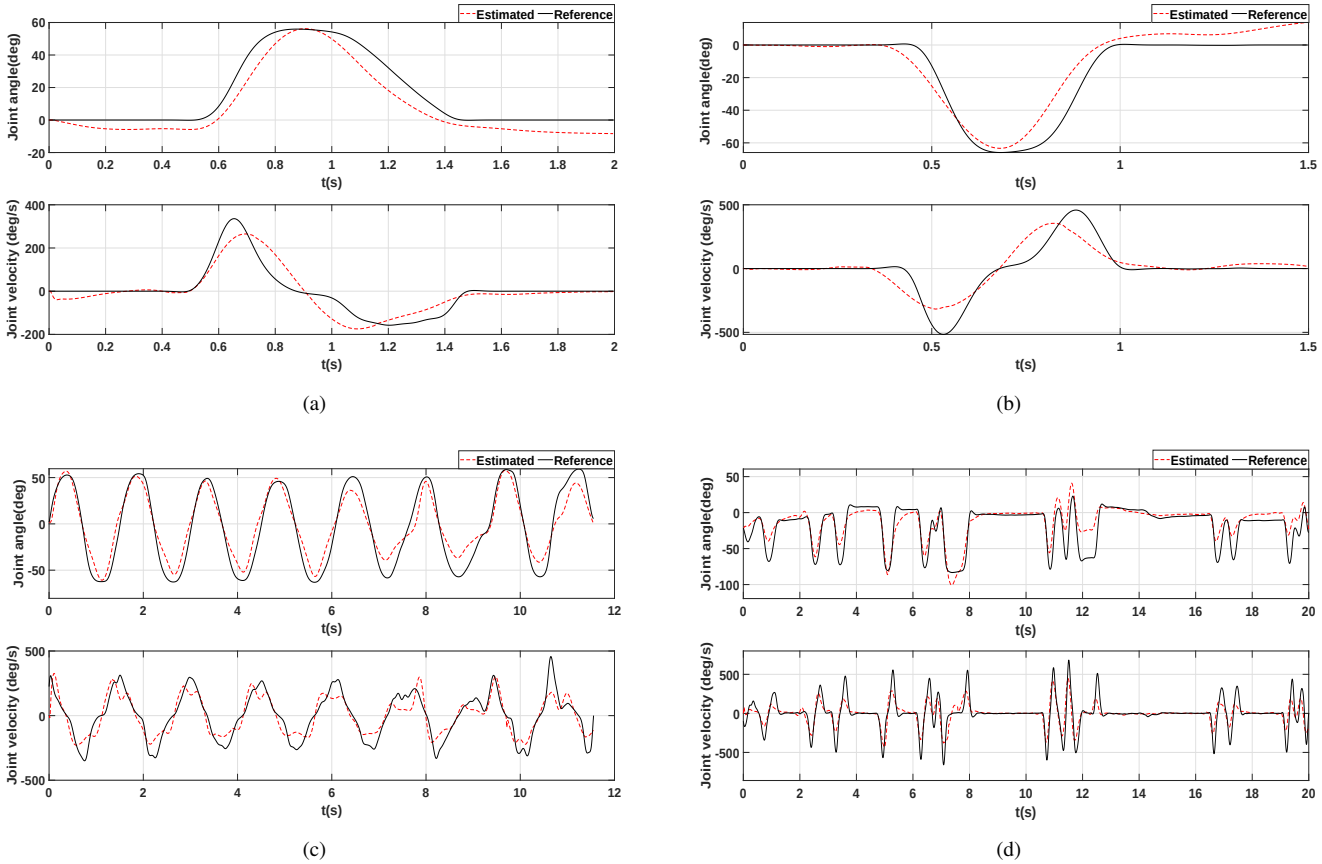

Fig. 5: Comparison between the estimated results (red dashed line) and the reference (black line) of 5(a) flexion ($R^2 = 0.985, \mathrm{RMSE} = 7.79^\circ$), 5(b) extension ($R^2 = 0.971, \mathrm{RMSE} = 8.49^\circ$), 5(c) continuous cycle motion ($R^2 = 0.972, \mathrm{RMSE} = 13.27^\circ$) and 5(d) random motion ($R^2 = 0.875, \mathrm{RMSE} = 14.87^\circ$) in subject four. In each panel, the estimated joint angle (top figure) and joint velocity (bottom figure) are presented.

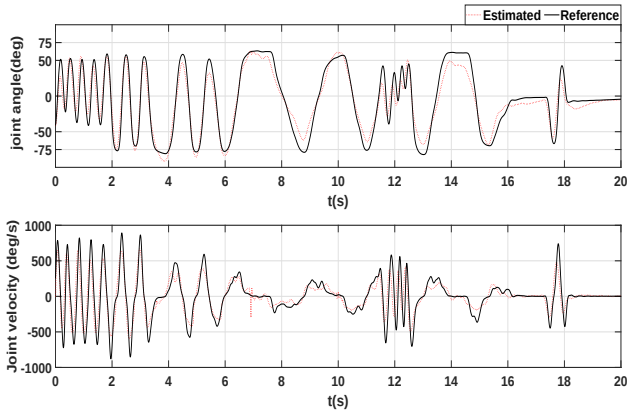

Fig. 6: The estimation result of one random trial in subject six. The R^2 and RMSE are 0.962 and 13.5° respectively.

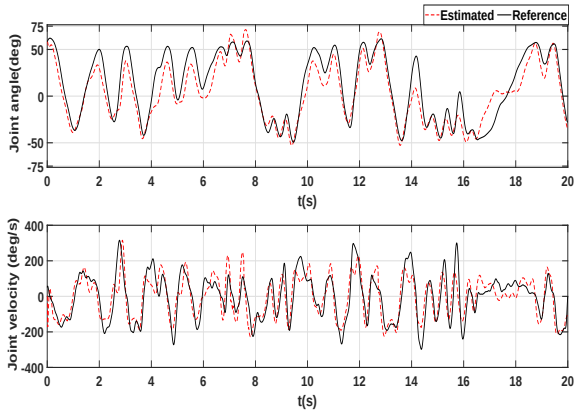

Fig. 7: The estimation result of one random trial in subject eight. The R^2 and RMSE are 0.937 and 14.6° respectively.

TABLE III: Optimized parameters of subject five

	Parameter index									
	$l^m_{o,i}$ (m)		$F^m_{o,i}$ (N)		l^t_i (m)		$\phi_{o,i}$ (rad)		k^{mt}_i	
Muscle index	Initial	Variation	Initial	Variation	Initial	Variation	Initial	Variation	Initial	Variation
FCR	0.062	101.40%	407	68.96%	0.24	103.90%	0.05	102.38%	1	96.38%
FCU	0.051	100.78%	479	92.33%	0.26	100.85%	0.2	99.73%	1	97.87%
ECRL	0.081	98.38%	337	73.77%	0.24	104.02%	0	NaN[1]	1	96.47%
ECRB	0.058	99.73%	252	136.03%	0.22	99.47%	0.16	97.79%	1	92.54%
ECU	0.062	98.86%	192	139.28%	0.2285	96.46%	0.06	96.61%	1	94.88%

[1] The denominator is zero. The optimized pennation angle of ECRL is $0.0399\,\mathrm{rad}$.

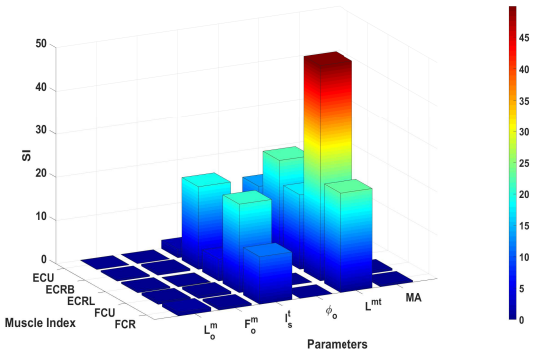

Fig. 8: Sensitivity analysis of subject five.

lumped-parameter model shows the mean RMSE of 0.94 for the wrist random motion trials of the able-bodied subjects [10]. However, the optimized parameters are over-estimated.

3) Parameters of the EMG-driven model: The optimized parameters are constrained within the physiological range, as shown in Table III. The proposed EMG-driven model uses five primary muscles of wrist joint [29], the effects of finger flexor/extensor are minimized by keeping the thumb and digits relaxed. The tendon length and the optimal muscle fibre length deviate slightly from the initial guess, indicating these parameters are not over-estimated.

According to the results of the sensitivity analysis, the proposed model has very low sensitivity to the pennation angle (SI $\approx 10^{-3}$), which is consistent with [30]. The model output has medium sensitivities to optimal fibre length, maximum isometric force, moment arm and non-linear shape factor. The sensitivities of the tendon length and the muscle-tendon length are very high in the proposed model, this is because these parameters determine the muscle fibre muscle length with respect to the joint angle. Using the regression algorithms to estimate the muscle-tendon length can only represent the average value from cadaver studies. State-of-the-art methods to determine the muscle-tendon length include using the biomechanical model API, e.g., OpenSim [31], or the highly accurate estimation model [32]. Nevertheless, using the regression algorithms to compute the muscle-tendon length can ease the computational burden when the musculoskeletal model is used in real-time [28].

The exclusion of the elastic tendon can also reduce the computational cost through alleviating the numerical stiffness in the muscle-tendon model. Other approaches have used a passive damper which is modelled in parallel with the CE to avoid computing the infinite muscle contraction velocity in the muscle-tendon model [8], or have used the implicit formulation of the musculoskeletal model to reduce the numerical stiffness [9], [28]. Nevertheless, the proposed model shows similar results in terms of R^2 compared with [28], by assuming the tendon is rigid without increasing the computational complexity.

Genetic algorithm is widely used in the Hill's muscle model and can avoid local minima using the physiological constraints. The average optimization time is around half an hour. The optimization time can be reduced by reducing the parameters for optimization based on the sensitivity analysis, e.g., optimal pennation angle.

4) Offline computation time: The processing time of the proposed model is measured by executing a 20-second continuous trial [10]. The mean computation time for the muscle activation interpretation method, the muscle-tendon model and the joint kinematic modelling technique are 68 ms, 390 ms and 690 ms respectively. The program is executed on a personal PC with quad-core processing unit (4.2GHz) and 16GB of RAM memory. The overall computation time of the proposed model indicates that it is feasible for real-time implementation, according to the real-time control constraints.

5) Limitations: The proposed EMG-driven musculoskeletal model is experimentally verified on wrist flexion/extension motion. Nevertheless, there are several limitations. Firstly, the grouped five primary muscles not only have the contributions to wrist flexion/extension, but also to other DoFs, i.e., ulnar/radial deviation. The proposed model has been validated only on healthy subjects, more experimental work is required to quantify the performance on patients with neurological diseases, i.e., stroke and cerebral palsy.

V. Conclusion

This paper proposes an EMG-driven musculoskeletal model to estimate the continuous wrist motion. Muscle activation levels are acquired from five primary muscles for wrist flexion/extension. The muscle-tendon model computes the muscle-tendon force and then the continuous joint motion is estimated via the joint kinematic modelling technique. The genetic algorithm is developed and implemented to obtain the subject-specific physiological parameters. The proposed musculoskeletal model shows an accurate estimation in the

wrist flexion/extension motion with the mean R^2 of 0.9 for all the motion trials. The mean RMSEs are 10.08°, 10.33°, 13.22° and 17.59° for single flexion/extension, continuous cycle and random motion trials, respectively.

Future work includes the qualitative evaluation of real-time application of the proposed model into our previous wrist rehabilitation robot [33]. In addition, the model will be extended to estimate continuous wrist motion with multiple DoFs.

REFERENCES

[1] J. Qi, G. Jiang, G. Li, Y. Sun, and B. Tao, "Intelligent human-computer interaction based on surface emg gesture recognition," *IEEE Access*, vol. 7, pp. 61 378–61 387, 2019.

[2] R. J. Downey, M. Merad, E. J. Gonzalez, and W. E. Dixon, "The time-varying nature of electromechanical delay and muscle control effectiveness in response to stimulation-induced fatigue," *IEEE Trans. Neural Syst. Rehabil. Eng.*, vol. 25, no. 9, pp. 1397–1408, 2017.

[3] D. Ao, R. Song, and J. Gao, "Movement performance of human–robot cooperation control based on EMG-driven hill-type and proportional models for an ankle power-assist exoskeleton robot," *IEEE Trans. Neural Syst. Rehabil. Eng.*, vol. 25, no. 8, pp. 1125–1134, 2016.

[4] Z. Lei, "An upper limb movement estimation from electromyography by using bp neural network," *Biomed Signal Process Control*, vol. 49, pp. 434–439, 2019.

[5] U. Côté-Allard, C. L. Fall, A. Drouin, A. Campeau-Lecours, C. Gosselin, K. Glette, F. Laviolette, and B. Gosselin, "Deep learning for electromyographic hand gesture signal classification using transfer learning," *IEEE Trans. Neural Syst. Rehabil. Eng.*, vol. 27, no. 4, pp. 760–771, April 2019.

[6] M. Sartori, D. G. Lloyd, and D. Farina, "Neural data-driven musculoskeletal modeling for personalized neurorehabilitation technologies (vol 63, pg 879, 2016)," *IEEE Trans. Biomed. Eng.*, vol. 63, no. 6, pp. 1341–1341, 2016.

[7] J. W. Pau, S. S. Xie, and A. J. Pullan, "Neuromuscular interfacing: Establishing an EMG-driven model for the human elbow joint," *IEEE Trans. Biomed. Eng.*, vol. 59, no. 9, pp. 2586–2593, 2012.

[8] E. K. Chadwick, D. Blana, A. J. van den Bogert, R. F. Kirsch *et al.*, "A real-time, 3-d musculoskeletal model for dynamic simulation of arm movements," *IEEE Trans. Biomed. Eng.*, vol. 56, no. 4, pp. 941–948, 2008.

[9] D. Blana, E. K. Chadwick, A. J. van den Bogert, and W. M. Murray, "Real-time simulation of hand motion for prosthesis control," *Comput Methods Biomech Biomed Engin*, vol. 20, no. 5, pp. 540–549, 2017.

[10] D. L. Crouch and H. Huang, "Lumped-parameter electromyogram-driven musculoskeletal hand model: A potential platform for real-time prosthesis control," *J Biomech*, vol. 49, no. 16, pp. 3901–3907, 2016.

[11] T. S. Buchanan, D. G. Lloyd, K. Manal, and T. F. Besier, "Neuromusculoskeletal modeling: estimation of muscle forces and joint moments and movements from measurements of neural command," *J Appl Biomech*, vol. 20, no. 4, pp. 367–395, 2004.

[12] D. G. Lloyd and T. F. Besier, "An emg-driven musculoskeletal model to estimate muscle forces and knee joint moments in vivo," *J Biomech*, vol. 36, no. 6, pp. 765–776, 2003.

[13] D. G. Thelen, "Adjustment of muscle mechanics model parameters to simulate dynamic contractions in older adults," *J. Biomech. Eng.*, vol. 125, no. 1, pp. 70–77, 2003.

[14] L. M. Schutte, "Using musculoskeletal models to explore strategies for improving performance in electrical simulation-induced leg cycle ergonomi," Ph.D. dissertation, 1993.

[15] F. E. Zajac, "Muscle and tendon: properties, models, scaling, and application to biomechanics and motor control." *Crit Rev Biomed Eng*, vol. 17, no. 4, pp. 359–411, 1989.

[16] J. W. Ramsay, B. V. Hunter, and R. V. Gonzalez, "Muscle moment arm and normalized moment contributions as reference data for musculoskeletal elbow and wrist joint models," *J Biomech*, vol. 42, no. 4, pp. 463–473, 2009.

[17] J. J. Craig, "Introduction to robotics: mechanics and control," Tech. Rep., 2005.

[18] A. Falisse, S. Van Rossom, I. Jonkers, and F. De Groote, "EMG-driven optimal estimation of subject-specific hill model muscle–tendon parameters of the knee joint actuators," *IEEE Trans. Biomed. Eng.*, vol. 64, no. 9, pp. 2253–2262, Sep. 2017.

[19] R. L. Lieber, B. M. Fazeli, and M. J. Botte, "Architecture of selected wrist flexor and extensor muscles," *J HAND SURG*, vol. 15, no. 2, pp. 244–250, 1990.

[20] K. R. Saul, X. Hu, C. M. Goehler, M. E. Vidt, M. Daly, A. Velisar, and W. M. Murray, "Benchmarking of dynamic simulation predictions in two software platforms using an upper limb musculoskeletal model," *Comput Methods Biomech Biomed Eng*, vol. 18, no. 13, pp. 1445–1458, 2015.

[21] C. Y. Scovil and J. L. Ronsky, "Sensitivity of a hill-based muscle model to perturbations in model parameters," *J Biomech*, vol. 39, no. 11, pp. 2055–2063, 2006.

[22] D. Stegeman and H. Hermens, "Standards for surface electromyography: The european project surface EMG for non-invasive assessment of muscles (seniam)," *Enschede: Roessingh Research and Development*, pp. 108–12, 2007.

[23] M. Masjedi and L. D. Duffell, "Dynamic analysis of the upper limb during activities of daily living: Comparison of methodologies," *Proc Inst Mech Eng H*, vol. 227, no. 12, pp. 1275–1283, 2013.

[24] K. Nizamis, N. H. Rijken, R. Van Middelaar, J. Neto, B. F. Koopman, and M. Sartori, "Characterization of forearm muscle activation in duchenne muscular dystrophy via high-density electromyography: A case study on the implications for myoelectric control," *Front. Neurol.*, vol. 11, p. 231, 2020.

[25] L. Pan, D. L. Crouch, and H. Huang, "Comparing EMG-based human-machine interfaces for estimating continuous, coordinated movements," *IEEE Trans. Neural Syst. Rehabil. Eng.*, vol. 27, no. 10, pp. 2145–2154, 2019.

[26] J. Han, Q. Ding, A. Xiong, and X. Zhao, "A state-space EMG model for the estimation of continuous joint movements," *IEEE Trans. Ind. Electron.*, vol. 62, no. 7, pp. 4267–4275, 2015.

[27] W. Wang, W. Shi, Z. Hou, B. Chen, X. Liang, S. Ren, J. Wang, and L. Peng, "Prediction of human voluntary torques based on collaborative neuromusculoskeletal modeling and adaptive learning," *IEEE Trans. Ind. Electron.*, pp. 1–1, 2020.

[28] D. Blana, A. J. Van Den Bogert, W. M. Murray, A. Ganguly, A. Krasoulis, K. Nazarpour, and E. K. Chadwick, "Model-based control of individual finger movements for prosthetic hand function," *IEEE Trans. Neural Syst. Rehabil. Eng.*, vol. 28, no. 3, pp. 612–620, 2020.

[29] M. Sartori, G. Durandau, S. Došen, and D. Farina, "Robust simultaneous myoelectric control of multiple degrees of freedom in wrist-hand prostheses by real-time neuromusculoskeletal modeling," *J. Neural Eng.*, vol. 15, no. 6, p. 066026, 2018.

[30] V. Carbone, M. van der Krogt, H. F. Koopman, and N. Verdonschot, "Sensitivity of subject-specific models to hill muscle–tendon model parameters in simulations of gait," *J Biomech*, vol. 49, no. 9, pp. 1953–1960, 2016.

[31] S. L. Delp, F. C. Anderson, A. S. Arnold, P. Loan, A. Habib, C. T. John, E. Guendelman, and D. G. Thelen, "Opensim: open-source software to create and analyze dynamic simulations of movement," *IEEE Trans. Biomed. Eng.*, vol. 54, no. 11, pp. 1940–1950, 2007.

[32] Massimo Sartori, M. Reggiani, A. J. van den Bogert, and D. G. Lloyd, "Estimation of musculotendon kinematics in large musculoskeletal models using multidimensional b-splines," *J Biomech*, vol. 45, no. 3, pp. 595 – 601, 2012.

[33] W. Meng, B. Sheng, M. Klinger, Q. Liu, Z. Zhou, and S. Q. Xie, "Design and control of a robotic wrist orthosis for joint rehabilitation," in *2015 IEEE International Conference on Advanced Intelligent Mechatronics (AIM)*, July 2015, pp. 1235–1240.